# "RAPID" Regions-of-Interest Detection in Big Histopathological Images

Li Yin Sulimowicz, Ishfaq Ahmad
li.yin@mavs.uta.edu, iahmad@cse.uta.edu
University of Texas Arlington — Department of Computer Science and Engineering

## Introduction

### Background & Goal

- The sheer volume and size of histopathological images is growing explosively (*e.g.*, $10^6$ MPixel).
- Regions-of-interest (ROI) detection in big image is just a preprocessing step, this underscores the need for faster speed.

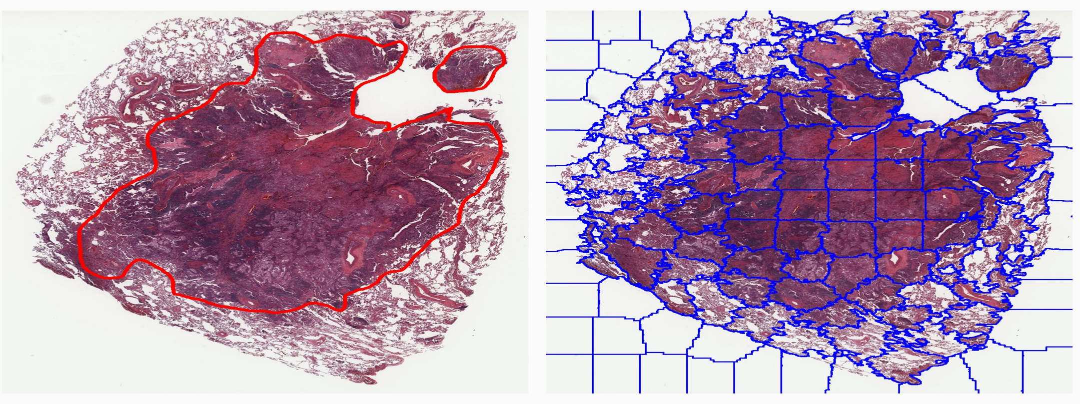

**Figure 1:** Ground truth (left); Result from [1]

### Discovers

- A coarse-to-fine algorithm [1] gained real-time complexity and is the fastest compared with the state-of-the-art algorithms.
- Only the precision of the boundary between ROI and non-ROI area decides the final accuracy.

## Baseline Method

Regular and Adaptive Prediction-Induced Detection (RAPID) is based on a multi-layer coarse-to-fine segmentation algorithm [1, 2].

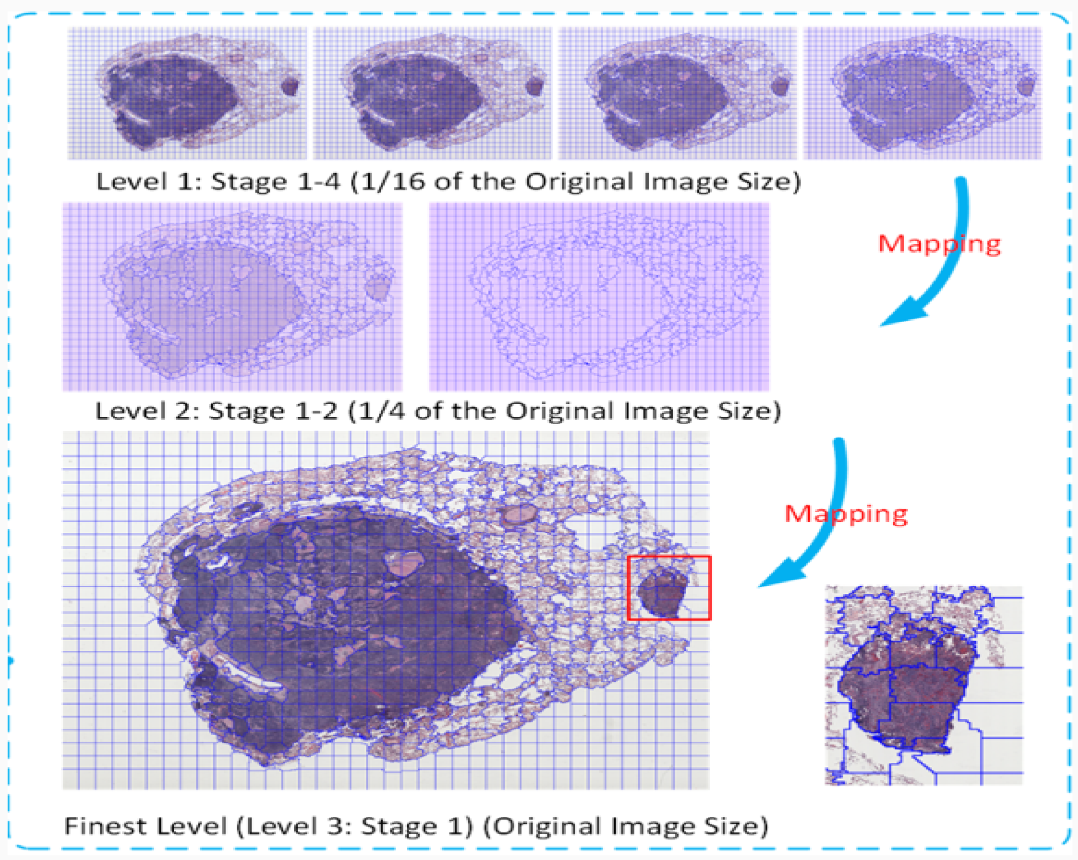


**Figure 2:** Multi-layer segmentation framework [2]

### Energy Function

$$E(\mathbf{s},\boldsymbol{\mu},\mathbf{c}) = \sum_p E_{col}(s_p, c_{s_p}) + \lambda_{pos}\sum_p E_{pos}(s_p, \mu_{s_p}) + E_{topo}(s) + \lambda_b \sum_p \sum_{q\in N_4} E_b(s_p, s_q) + \lambda_s E_{size}(s) \quad (1)$$

**Boundary blocks:** block which has at least one neighbor that has a different superpixel label.

$$E_b(s_p, s_q) = \begin{cases} 1, & s_p \neq s_q, \\ 0, & otherwise. \end{cases} \quad (2)$$

## Method

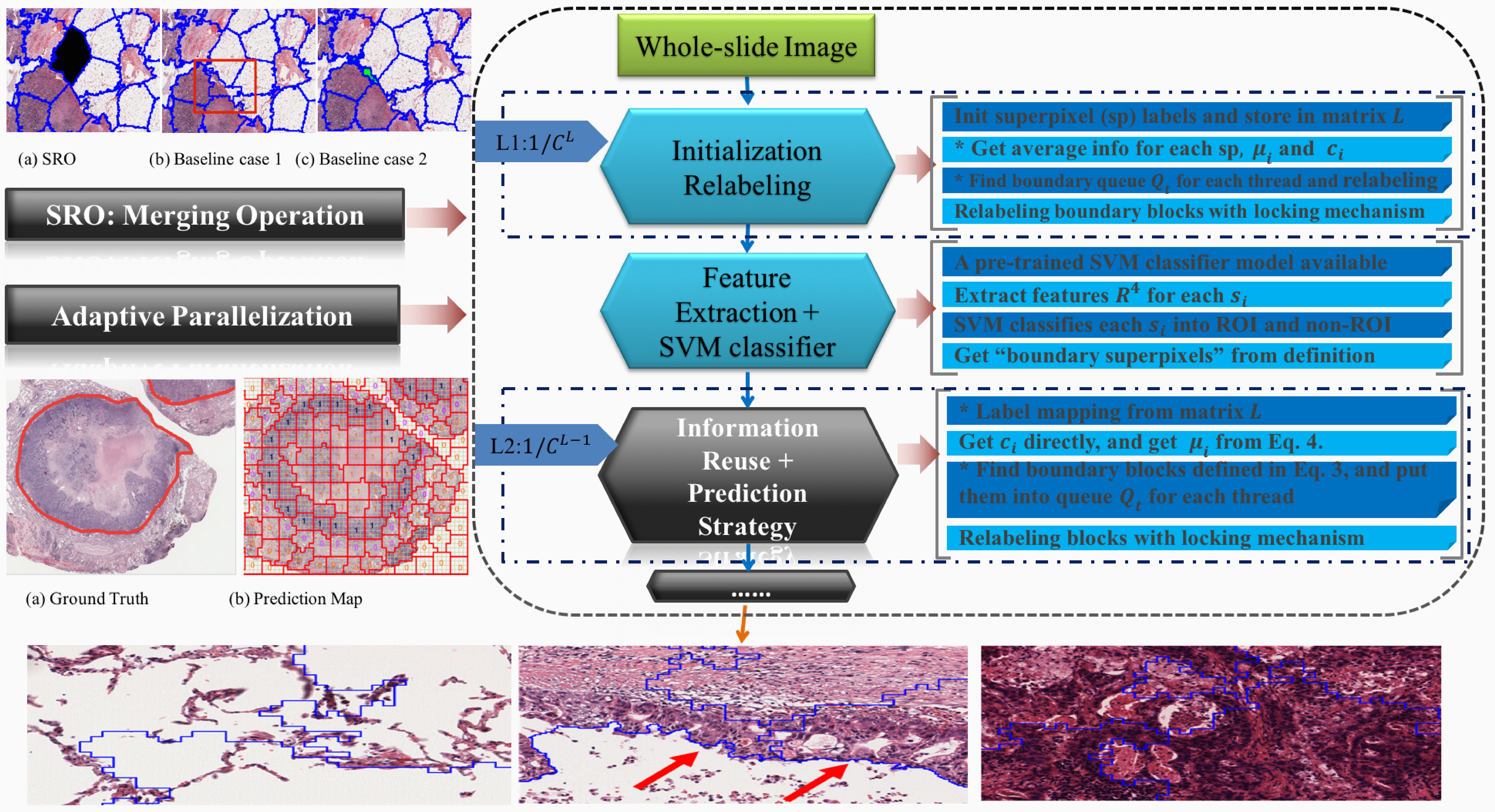


**Figure 3:** Parallel "RAPID" arithmetic flow, the steps marked with ⋆ is trivially parallelization; For the bottom figure, coarse segment in non-ROI and ROI (left and right); fine segment at the boundary (middle).

⋆ **Superpixel Regularity Optimization (SRO):** defines a merging operation. When the superpixel size after moving a block $p_i$ from $s_{p_i}$ is smaller than a lower threshold, SRO searches another neighbor superpixel $s_{p_m}$ with conditions: 1) minimum gross energy; 2) $Size(s_{p_m}) < \mu InitSize$, $\mu$ is the upper bound.

⋆ **Information Reuse:** The average brightness information for each superpixel is directly passed to the next level. The position information is converted with Eq. 3.

$$\mu_{i+1} = C \times \mu_i - \frac{C-1}{2} \quad (3)$$

$C$ : compression ratio, $i$ : image level

⋆ **Prediction Strategy:** "Boundary superpixel" (shown in left bottom Fig 3, purple 0 and the blue 1) is a superpixel that is classified as ROI or non-ROI, and has at least a neighbor which is classified otherwise.

$$E_b(s_p, s_q) = \begin{cases} 1, & s_p \neq s_q, y_{s_p} \neq y_{s_q}, \\ 0, & otherwise. \end{cases} \quad (4)$$

Newly defined boundary blocks decreases the size of the boundary queue.

⋆ **Parallelization Scheme:** evenly splits the rows in image. Use locking mechanism on the superpixel average info vector when relabeling.

$$startR = totalR * i/totalThreads \quad (5)$$
$$endR = totalR * (i+1)/totalThreads$$

## Results

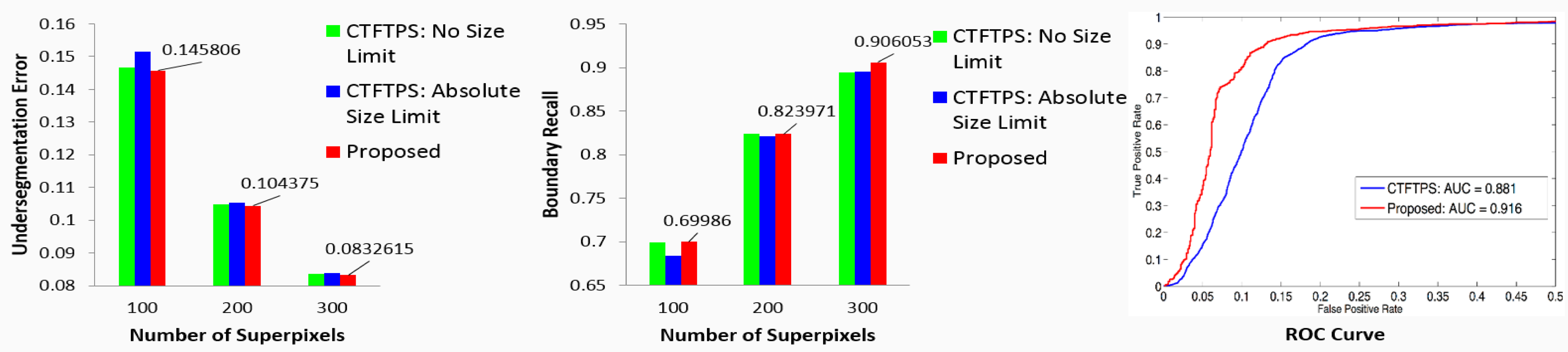


**Figure 4:** Comparison between CTFTPS with and without superpixel regularity optimization.

**Table 1:** Comparison of the average time cost.

| Average Image Size | Grain | SLIC | CTFTPS | Multi-CTFTPS | **RAPID** |
|---|---|---|---|---|---|
| 4712 × 5867 | 1 × 1 | 12.90$s$ | 3.29$s$ | 3.54$s$ | **1.56s** |
| 23561 × 29335 | 4 × 4 | N/A | 27.26$s$ | 28.98$s$ | **6.96s** |
| | 1 × 1 | 809$s$ | 79.46$s$ | 66.46$s$ | **17.54s** |

**Table 2:** Average time cost of Parallel RAPID with different number of threads.

| Average Image Size | Grain | 2T | 4T | 8T | 14T | 24T |
|---|---|---|---|---|---|---|
| 4712 × 5867 | 1 × 1 | 1.09$s$ | 0.63$s$ | 0.49$s$ | 0.42$s$ | 0.34$s$ |
| 23561 × 29335 | 4 × 4 | 4.39$s$ | 3.79$s$ | 1.95$s$ | 1.69$s$ | 1.54$s$ |
| | 1 × 1 | 12.13$s$ | 7.83$s$ | 6.29$s$ | 5.83$s$ | 5.20$s$ |

Parallel RAPID gained 13 times speedup compared with [1], and around 160 times with SLIC.

## References


[1] Jian Yao, Marko Boben, Sanja Fidler, and Raquel Urtasun. Real-time coarse-to-fine topologically preserving segmentation. 2015.

[2] Ruoyu Li and Junzhou Huang. Fast regions-of-interest detection in whole slide histopathology images. 2015.